JOURNAL OF
EMERGING INVESTIGATORS

Article

# Cleaning up the world's oceans with underwater laser imaging

**Mustafa Alperen Gurbuz[1], Seongsin Kim[2]**

[1] Northridge High School, Tuscaloosa, Alabama

[2] Department of Electrical and Computer Engineering, The University of Alabama, Tuscaloosa, Alabama

## SUMMARY

**It is estimated that there are 5.25 trillion pieces of plastic waste in the oceans. Of this plastic, roughly 70% is not visible because it is underwater. This plastic is harmful to animals as they can get entangled in the litter and ingestion of plastic toxins can cause disease. Although cameras and hyperspectral imagers have been used to find plastics in the ocean, their efficacy is limited to visible garbage on the ocean surface. Ocean cleaning up requires retrieval of not just visible garbage, but underwater garbage as well. For this task, both sonar and Light Detection and Ranging (LIDAR) can be utilized; however, sonar can be harmful to marine animals by disrupting their echolocation capabilities. LIDAR generates high resolution point clouds with which recognition of small objects may be difficult. Therefore, we investigated the ability of lasers to image and identify underwater objects. Laser imaging can penetrate underwater, providing informative images at depths where there is no ambient light. This study examined the influence of various factors on underwater laser image quality: polarization, depth, turbidity, and object material. We conducted experiments by illuminating objects in water with a laser and recording illuminated objects using a camera. We utilized various image processing techniques to enhance image quality. Our results show that deconvolution was a more effective method than alternatives for reducing blurriness and that laser imaging is a viable method for detecting underwater garbage.**

## INTRODUCTION

It is estimated that there are 5.25 trillion pieces of plastic waste in our oceans (1). Although the Great Pacific Garbage Patch may be the most well-known repository of trash in the ocean, it is just one of five garbage patches worldwide. While 8.3 million tons of plastic are discarded in the sea yearly, only 15% of this amount floats. Another 15% washes ashore on our beaches, and the remaining 70% sinks to the bottom of the ocean's ecosystem, resulting in 4 billion microfibers per $km^2$ below the surface (2).

Plastic waste in oceans is harmful to sea life. One hundred million marine animals die each year from plastic waste, and fish ingest 12–14 thousand tons of plastic waste yearly (3). Not all deaths are caused by ingestion; many animals die from getting entangled in the litter. Worse, some animals end up living extended durations of time intwined in the plastic. Although some have tried to free animals like sea turtles from plastic straws stuck up their nostrils or soda can plastics tightly wrapped around their neck, thousands of other creatures continue to suffer from trash in the oceans (4). Moreover, when micro-plastics degrade due to sun exposure and wave action, the chemicals released in the process of degradation contaminate the ocean (5,6). These contaminates, such as lead, cadmium, and mercury, enter the human food chain as well. Humans consume these toxins when eating contaminated fish and mammals. Bottle caps and other plastics have been found in the stomachs of birds and fish who have died and washed ashore (7). Many plastic toxins have been directly linked to cancer, birth defects, immune system problems, childhood developmental issues, and disrupted hormonal function (8).

Thus, while many in the world are aware of the dangers to human and animal welfare posed by degrading plastics and resulting toxicity, simply eliminating the use of plastic is not enough. As a society, we must embrace the task of cleaning up as much plastic as possible in the oceans to prevent continuing contamination of our food chain and water supply.

Due to the harmful effects of plastics in the ocean, there has been an effort to clean up the ocean by gathering up the garbage using nets and large sea barges. Although this method allows us to clean the 15% of surface trash on the ocean, the vast majority remains below the surface and not visible (1). Thus, a technique for detecting and recognizing objects underwater is needed to discover the location of ocean garbage so it can be removed from the water.

There are multiple ways to be able to detect the garbage. The main three ways are to use cameras, sonar, or Light Detection and Ranging (LIDAR). Cameras have the capability of providing high-resolution images for object recognition, but they are ineffective underwater because little visible light penetrates the ocean surface, especially at the deeper depths where much garbage can be found. While red light disappears in water at a range of 4.57 m, orange after 9.14 m, yellow after 18.29 m, and green after 24.39 m, most cameras are not effective at recognizing objects at ranges beyond 15 m underwater (9,10). Alternatively, sound navigation and ranging (sonar) can be utilized deep in the ocean. Sonar operates by transmitting an acoustic signal and acquiring the backscatter from objects in the water. Based on the round-trip travel time of the signal, sonar can determine the distance of an object. Typical sonar systems, such as those used by a submarine, can achieve a maximum detection distance of about 5.8 km and 8.4 km, depending on whether it is summer or winter, respectively (11). However, sonar cannot easily differentiate between sea life and objects, such as fishes and garbage. It can only detect whether an object is present and which direction it is moving because the shape of an object in a sonar image is affected by the direction from which the

object is observed relative to the direction of motion (12). Moreover, sonar can negatively affect the health of marine animals, especially whales and dolphins, by disrupting their understanding of location and direction (13). Sonar can also interfere with dolphins mating, separate calves from mothers, inflict physical injuries like ear damage and temporary damage to echolocation abilities, and in rare cases, cause death (14). As another example, to avoid the disruptive effects of sonar, whales may either beach themselves or rapidly dive deep, which can cause bleeding from the ears and eyes and pain (15,16).

In contrast, LIDAR, a device that uses pulsed lasers to measure the distance to an object or surface by measuring the time for the reflected light to return to its receiver, has the advantage that it can penetrate the water while using low frequency beams to detect objects with potentially less disruption to marine life (17). There has been an increasing amount of research involving the use of lasers underwater, such as for applications of underwater mapping, communications, and Internet of Underwater Things (IoUT) (18-20). Lasers have also been used by scuba divers to illuminate the underwater environment and communicate with other divers (21). These applications use Class III or IV lasers, which raises concerns over how the laser light might impact marine life (22). One recent study determined that if the human eye is not harmed, then the eyes of cetaceans, such as dolphins and whales, or pinnipeds, such as seals, would also not be harmed (23). The authors recommended avoiding laser illumination of groupings of marine animals and disengaging the laser if encountered (23). In the case of underwater laser imaging, the power of the laser impacts the distance an object can be effectively imaged (24). The requirements on laser power can be minimized by designing more sensitive optical detectors or by improving the image processing algorithms so that objects can be detected at greater distance with lower power. Using a lower power laser in a scanning mode would minimize potential impact on marine life by reducing the likelihood of the laser beam directly contacting the eye of a marine animal at a power level that would be dangerous.

LIDAR technology has been used for underwater sea surveys, contributing to environmental science and conservation, as well as mapping the depth of the ocean floor and surveying sea habitats (25,26). In 2019, Kraken Robotics developed a compact, underwater laser imaging system that could generate dense 3D point cloud images - a collection of points that reveal the surface of an object - of plant and animal life in the ocean (27). It was designed for deployment on an underwater robotics platform. Because of the time required by underwater vehicles to survey and scan large volumes of ocean, there has recently been research into mounting LIDAR sensing systems on unmanned aerial vehicles (UAVs). Although airborne LIDAR system are degraded by the strong reflections of sunlight from the water's surface, last year, one proof-of-concept study conducted over shallow coastal areas integrated a LIDAR onto a UAV and showed that it could be possible to detect objects beneath the water's surface in real-time (23).

LIDAR point clouds reveal the general shape of an object, but to identify whether an object is garbage and to avoid confusion with fish, kelp, or other sea life, it would be better to have an actual image of the object. Lasers, the core technology of LIDAR, can also be used for underwater imaging (28). Because lasers actively transmit their own source of light, the power of the laser can be adjusted to achieve greater penetration and to image objects at greater depth. Also, if the laser were mounted on an underwater robot, the active illumination of LIDAR can enable acquisition of much deeper objects. In this case, the power of the laser would determine the maximum distance between the object and underwater vehicle at which images could be obtained. However, different factors may affect the quality of underwater images (29).

The objective of this research was to investigate the impact of various factors on underwater laser imaging. For this, we determined how the resolution of laser imaging will change with depth and turbidity, how the polarization of a laser effects image resolution quality and how image processing can be used to enhance underwater laser images. We hypothesized that both depth and turbidity of the water would result in the images becoming fainter and blurrier, making it harder to identify objects. We also hypothesized that different polarizations may bring out different features of the images, which may improve our ability to recognize the objects. Because there has been much work on the removal of atmospheric haze and blurriness in aerial photos, we were curious about their efficacy on underwater laser images (30). Thus, we implemented three common noise-reduction and deblurring algorithms - guided filtering, de-hazing, and blind deconvolution - and compared their efficacy. Based on our visual observations and analysis of the images, we found that underwater laser imaging is a viable method for detecting garbage underwater and conclude by discussing implications for future work.

## RESULTS

The efficacy of underwater laser imaging was evaluated by conducting experiments in a laboratory using a green laser and objects submerged in a 4 ft long glass aquarium. To be able to better design our experiment, we first used the LIDAR range equation to predict how much the backscatter in the water column reduces the intensity picked up by the camera. Next, we acquired laser images for objects of different size and material composition at different depths in water with different turbidity levels using the laser adjusted for linear and circular polarization. Inspecting the images, we visually observed the impact of depth, turbidity, and polarization on the images. We then implemented several different deblurring methods to try to improve the clarity of objects in the laser images we acquired. We based our results on visual as well as quantitative analysis of the images with respect to our research variables.

### Theoretical Analysis

The LIDAR range equation provides a theoretical model for the expected received power, which determines the intensity of pixel values, to the detector from the transmitted beam of the laser (31). In general, an overall model of the expected received optical power given interaction with an object in the water tank can be expressed as:

$$P_r = \frac{P_t D_r^2 \eta}{\pi (n_w H + D)^2} \cos(\alpha) \times WR_b \times e^{-2KD} \quad \text{[Eqn. 1]}$$

where $P_t$ is the transmitted power in watts, $D_r$ is the receiver aperture diameter in $m$, η is a transmission factor,

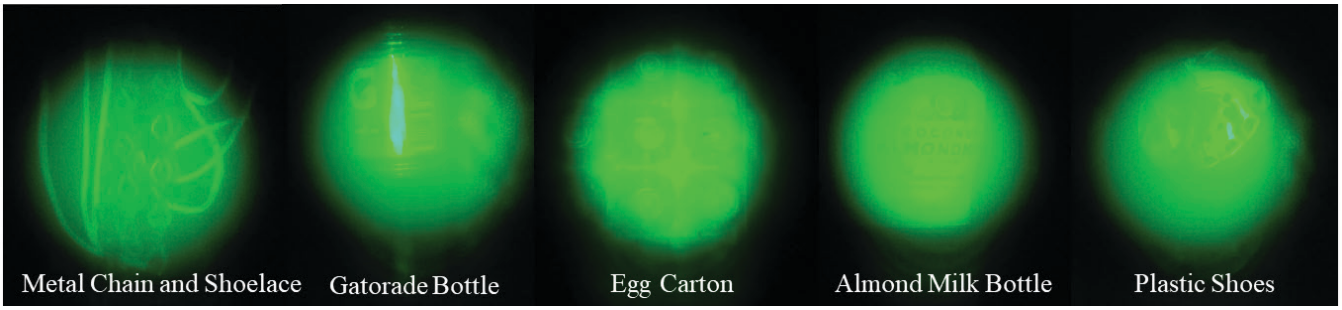


**Figure 1: Effect of material on laser images in clear water under linear polarization.** The transparent Gatorade bottle reflects much more compared to other material, such as the plastic shoes. The writing on the Almond Milk Bottle is more clearly visible because of the contrast of colors. Even though metal is a better reflector than shoelaces in air, the shoelace is much more reflective than the metal chain underwater.

*H* is the distance traveled in the air in m, *W* is a combined factor representing loss factors, $R_b$ is the benthic reflectance, *K* is the diffusive attenuation coefficient of water, and *D* is the benthic depth. Object reflectivity typically depends on the amount of light absorbed by the object's material at the laser's wavelength, the incidence angle ($\alpha$) at which the laser beam interacts with the object, the solid angle of the backscatter and the area of the object. This equation also assumes that the entire laser beam interacts with the object (in other words, the object is wider than the beam extent for the distance at which the target is located) and that the object backscatter is the same in every direction.

Since our experiment was conducted in a glass tank, unlike real-world ocean sensing, we were also required to take into consideration the potential impact of the glass on the laser beam. As the beam passes through the glass wall of the water tank, the laser beam refracted at the air-glass and glass-water interfaces. According to Snell's law, the angle of refraction as the beam passes through an interface is $n_1 sin(\theta_t)=n_2 sin(\theta_2)$, where $n_1$ and $n_2$ are the refractive indices of the respective media, and $\theta_1$ and $\theta_2$ are the angles of incidence. If the angle of incidence of the LIDAR beam is perpendicular to the interface, as is the case in our experimental set-up, there were no change in the angle of incidence of the LIDAR beam as it passed through the glass interface. Therefore, no refractive effects were needed to be added into Equation 1 for this experiment.

Based on Equation 1, because the length of the water tank is 1.2 m, when an object is placed at the furthest end of the tank, the beam will have a round-trip travel distance of about 2.4 m, resulting in an overall degradation factor of 0.01. In other words, the water column decreases the strength of the optical power by a factor of 100 when the object is furthest. When an object is placed in the center of the tank, so that the distance is halved, the degradation factor is about 0.15. Based on this analysis using the LIDAR range equation, it is expected that distance will greatly reduce the received power and therefore contrast in the image, eventually making objects undetectable as distance increases.

## Qualitative Observations

Objects made from different materials can have different levels of reflectivity. To test the effect of material on the laser image of an object, we compared the images of objects that are metal, clear or painted/opaque plastic, fabric, Styrofoam and rubber at the same depth, linear polarization and zero turbidity (clear, fresh water). The plastic bottles appeared to be highly reflective, and many images had glare in them **(Figure 1)**. The writing on the milk bottle is easily readable, while color changes, such as that on the small plastic shoes, are easily visible. The metal chain appeared subdued relative to the shoelace, which, in contrast, was quite bright.

As the depth of objects increased, the blurriness of the image also increased, causing finer features to become obscured **(Figure 2)**. At a depth of 76.2–91.44 cm, only the outline of an object was barely visible. This was consistent with our estimates made based on Equation 1 where we

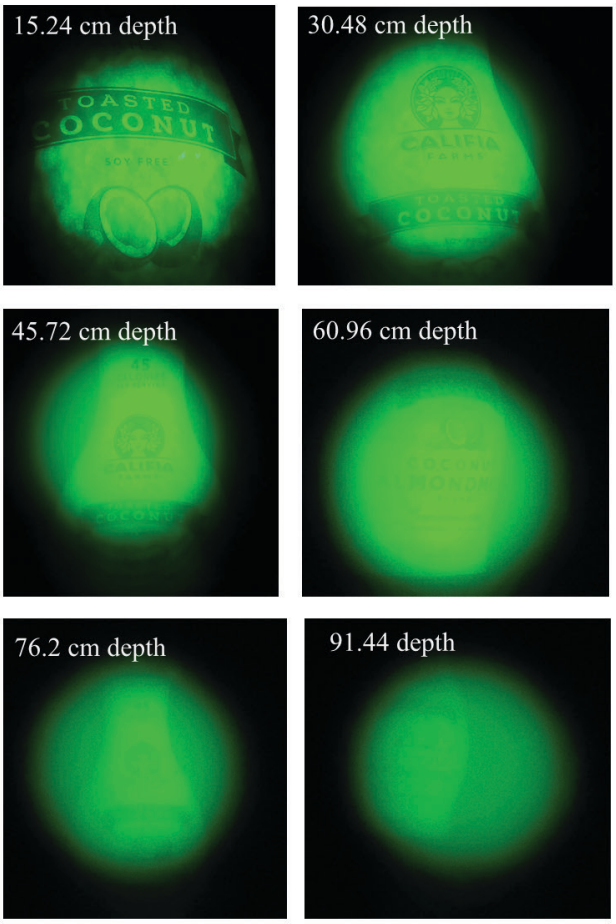


**Figure 2: Almond milk bottle under linearly polarized laser in clear water.** As the depth of the object from the camera increases, blurriness also increases.

found that at 1.22 m the water column resulted in a power attenuation factor of 0.01.

To investigate the impact of polarization on image quality, we compared the images for objects at a depth of 45.72 cm when illuminated with laser light of linear and circular polarization. Polarization determines the geometric orientation of light waves. For example, linearly polarized light waves oscillate back and forth along a line, while circularly polarized light waves rotate with respect to the direction of travel. The backscatter from different materials changes depending on polarization. For some objects such as the milk bottle and the Gatorade bottle, linear polarization yields images with greater contrast **(Figure 3)**. This is evident because with linear polarization, the writing on the milk bottle was clear, while the outline of the Gatorade bottle was also distinct. In contrast, these edges were not clear in the circularly polarized images. The image of the egg carton also exhibited greater contrast under linear polarization, while there was less variation of pixel intensities in the circularly polarized. However, for objects such as the metal chain and shoelace, circular polarization provided a clearer image relative to linear polarization. This is evident by the rings of the metal chain being more visible under circularly polarized laser illumination. From observations comparing the egg carton and metal chain under linear and circular polarization, we inferred that the material of the object is an important factor in laser imaging efficacy, as is the polarization of the laser **(Figure 3)**.

To test the effect of turbidity, we added calcium bentonite, a white powder used in making facial creams that has no known adverse effects on human health, to the water. The powder resulted in a turbidity so high that it was only at a depth of 15.24 cm that any part of the milk bottle and small plastic shoes could be visible **(Figure 4)**. We found it interesting that the writing on the milk bottle could be so visible while the egg carton appeared completely blurry. This could be in part due to the greater extent to which the material and shape of the egg carton disperses light.

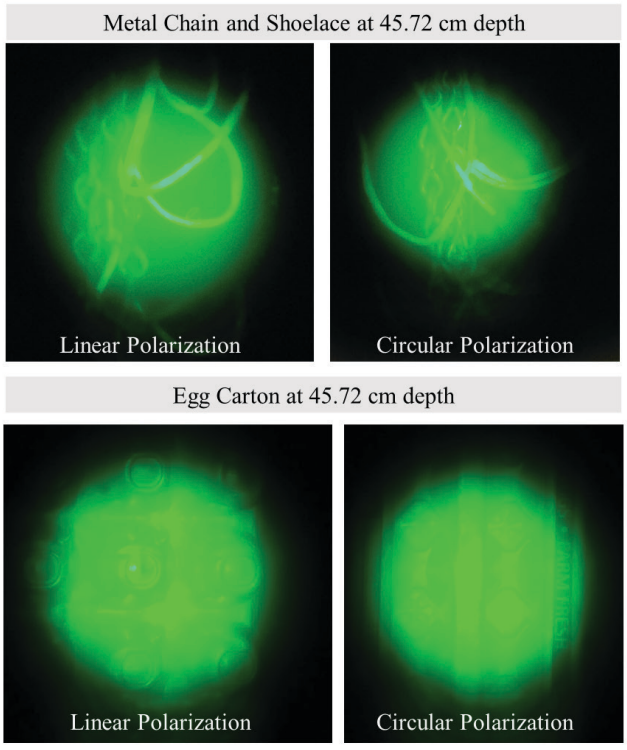


**Figure 3: Examples comparing circular and linear polarized images.** The metal chain looks clearer under circular polarization, while the egg carton has greater clarity and contrast under linear polarization.

## Quantitative Evaluation

We assessed the impact of variables, such as depth, polarization, and turbidity, by comparing the similarity between images when only one variable changes at a time. We utilized two metrics commonly used in image evaluation for this purpose: mean square error (MSE) and structural similarity index (SSI) (32). The MSE computes the average squared difference in digital number value between two pixels. In contrast, the SSI considers the relational properties between pixels locally. Consequently, the MSE can be highly affected by differences in orientation of the same object, while the SSI is a bit more robust to this factor. If two images are similar, the MSE value will be low, but the SSI value will be high (33).

We used the MSE and SSI to quantify the impact of linear versus circular polarization at different depths for all objects. We observed that the MSE exhibits much greater variance than the SSI. This reflects the sensitivity of MSE to the orientation of the object, because the MSE computation involves direct subtraction of pixel-to-pixel intensities squared. The SSI plots were much more consistent and less affected by orientation **(Figure 5)**. The SSI plots revealed the general trend that as the depth increases (irrespective of polarization) the SSI decreases. Lower SSI implies that there is less similarity. This is what we expected, as the increasing blurriness and lower signal-to-noise ratio (SNR) seen with increasing depth renders it less like the image at 15.24 cm.

To reduce the effects of blurring, which increases with depth and turbidity due to the increased backscatter of the water column, we implemented three different image deblurring methods: guided filtering, dehazing, and blind deconvolution (34-36). We compared the resulting image quality for the case of the almond milk carton illuminated with a linearly polarized laser located at a depth of 91.44 cm. Although the original image had a granular texture, we found that after guided filtering, the background and texture of the object was smoother and the MSE and SSI values also indicated slightly improved image quality **(Figure 6)**. However, this improvement was not practically significant, as it was still impossible to read the text on the milk bottle. We then experimented with dehazing, comparing the effect of the order in which the algorithms were applied on the data: first doing guided filtering and then dehazing or first doing dehazing and then guided filtering. Comparing the similarity metrics for these cases, we found that that first applying guided filtering followed by dehazing is slightly more effective than vice versa **(Figure 6)**. Neither guided filtering nor dehazing produced significantly tangible benefits towards enhancing the image sufficiently so the text on the milk bottle could be read.

We found that deconvolution yielded the most promising results. When we applied deconvolution to an image of the almond milk bottle for a depth of 45.72 cm and linear polarization, we saw a definite improvement in the crispness

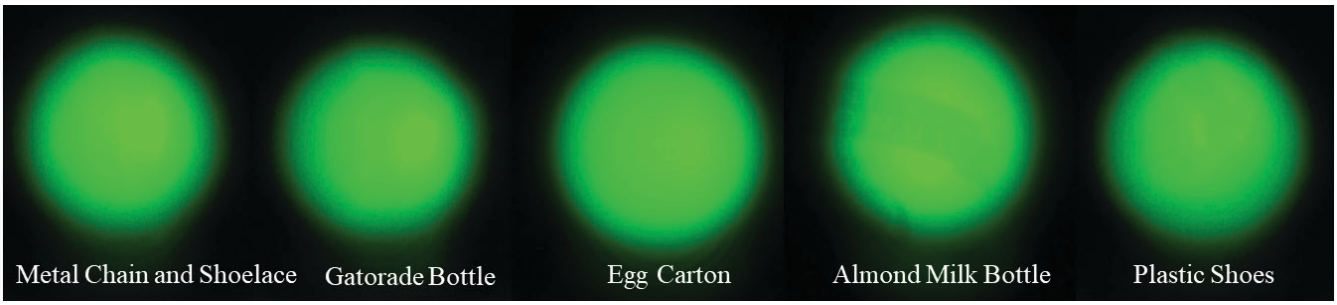


**Figure 4: Effect of high turbidity on visibility of objects at a depth of 15.24 cm.** Because of the high levels of turbidity in the water tank, many objects are not visible even at close ranges. The only object visible is the Almond Milk Bottle, because of the high contrast in color of its label.

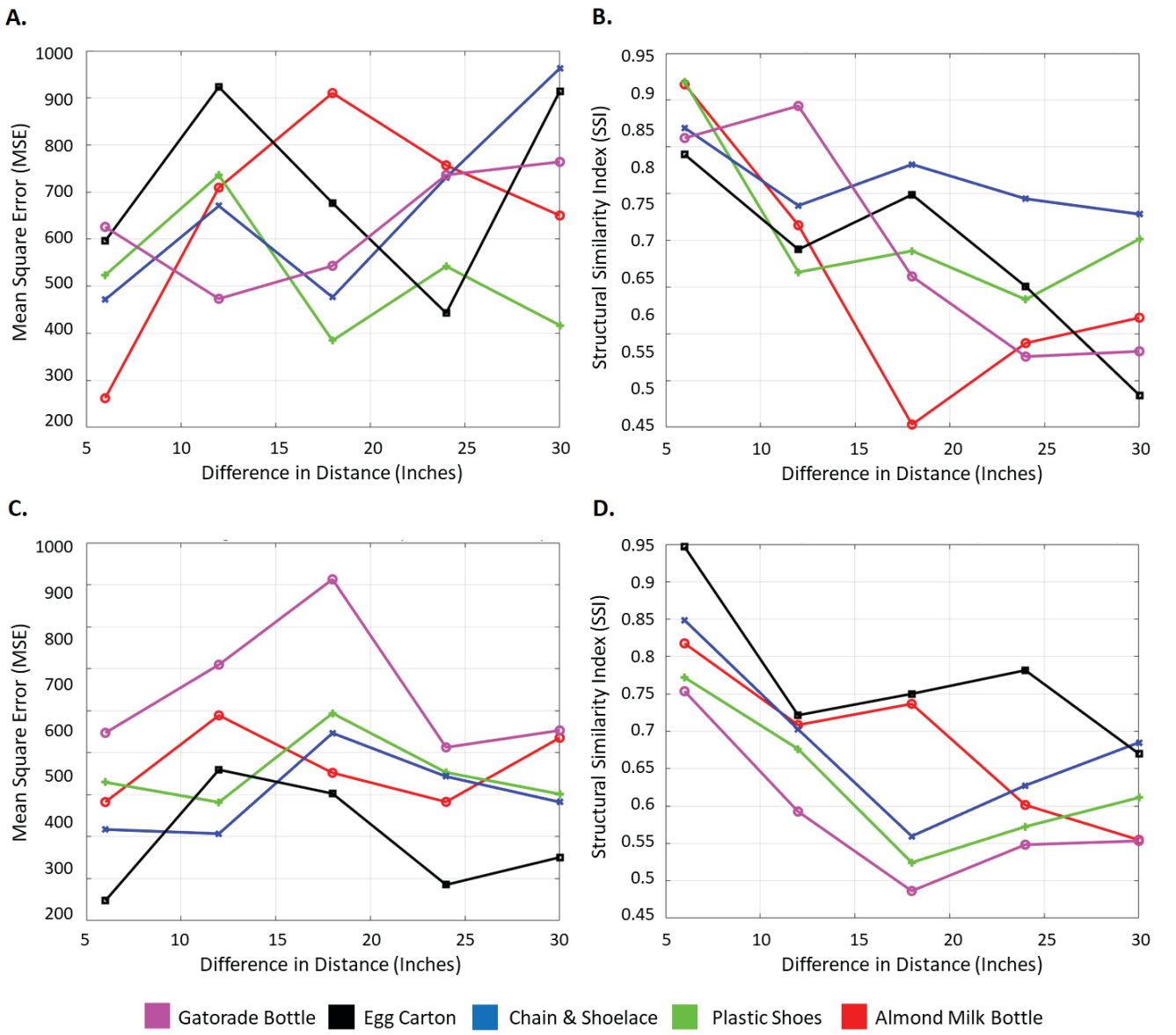


**Figure 5: Variation of MSE and SSI under linear and circular polarization. A)** MSE under linear polarization, **B)** SSI under linear polarization, **C)** MSE under circular polarization, and **D)** SSI under circular polarization with depth. MSE values fluctuate greatly with depth because MSE is computed pixel by pixel. As the perspective of the object in the image changes pixel by pixel changes are created. Thus, MSE as a metric has disadvantages. SSI on the other hand, is based on capturing object shape; therefore, we can observe a downward trend of similarity with distance, as expected, due to the increased blurriness in the image.

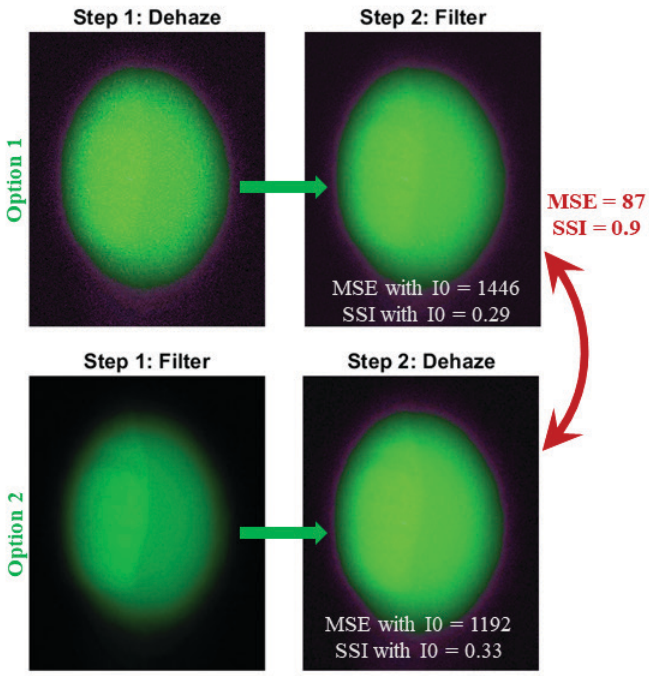


**Figure 6: Effect of image dehazing and noise filtering.** Regardless of the order with which dehazing and filtering are applied, the resulting images remained blurry.

of lines and readability of the text can be observed. However, we found that the efficacy of deconvolution changed according to the depth of the object. When we applied the same deconvolution function to an image of the milk bottle at 91.44 cm, however, no visible improvement was seen – the image was still blurry.

In summary, we acquired 277 underwater laser images in a lab setting using a 4 ft aquarium for different object depths and materials, water turbidity levels, and laser polarizations, and used this dat as the basis for our visual comparisons and quantitative analysis. We applied three different deblurring algorithms on these images and compared MSE and SSI values to better understand how image quality depends upon the experiment variables and on the type of image deblurring algorithm utilized to enhance the images.

## DISCUSSION

Overall, our results showed that using lasers to recognize objects underwater is possible, but that there are limitations on the conditions under which it can be effective. Different materials exhibit differences in backscatter, which can improve or degrade visibility. Polarization can reveal different features of the same image. For some materials, circular polarization resulted in clearer images, while for others linear polarization resulted in sharper images. Object depth is a significant factor impacting the quality of images. The deeper the object, the blurrier the image. We believe that this is due to the dispersion and backscatter of light by the water column itself, a problem that is even further compounded when the water is turbid. None of the image processing methods we tested were able to give clear images when the water is turbid. While turbidity may not be as big of a problem in the open ocean, along the coastline, sand and sea week will challenge laser image-based object recognition – we cannot see what light blocks.

We found that neither guided filtering nor dehazing were effective for deblurring laser images. Guided filtering smooths the image, and although the method tries to preserve edges, it does not really aim to improve sharpness. Dehazing, on the other hand, estimates radiometric transmission based on the properties of atmospheric propagation, not underwater propagation, which has different physics-based relationships. We believe that for this algorithm to be more effective on laser images, the transmission models would need to be revised for the underwater case. We found blind deconvolution can be a promising method for deblurring, even though we found that our implementation of deconvolution only worked at a certain depth. We believe that this is because the deconvolution method relies on having a mathematical model or estimate of the impact of the water. Because the amount of backscatter of the water column changes with depth, the blurring model will also change. However, our implementation utilized a Gaussian model for the water. When this model is not a good match, the method will be ineffective. That an improvement was seen for any depth, however, means that with further research on modeling, this approach can be improved to give better results over a wider range of conditions.

In retrospect, there were several ways in which these experiments could have been more effectively conducted. First, we could have introduced the calcium bentonite more incrementally so that we could better control the turbidity level. When too much of the powder was added into the water tank at the beginning, making the water extremely opaque, there was no way of undoing the process and subsequently reducing the turbidity. Only a small, measured amount of the powder should have been added so that varying levels of turbidity could be assessed.

Second, the difference in orientation of the objects caused by the way the objects were manually held underwater introduced numerical errors in the similarity metrics due to the change in orientation. A better experiment could have been constructed by devising a mechanism for holding the objects underwater, rather than just having a person submerge the objects. Use of a fixed holder would have allowed consistency in the measurements and yielded more meaningful comparisons based on the similarity metrics.

In conclusion, we found that increasing depth and water turbidity are significant causes of increased blurriness in both linearly and circularly polarized laser images. But the use of image processing methods, such as deconvolution, can be helpful in decreasing blurriness and improving the resulting image clarity. More work on developing advanced image enhancement techniques can expand the real-world conditions under which objects can be recognized underwater. For example, a recent review paper on underwater image enhancement describes many new deep learning-based techniques that have achieved success with regular camera photos (37). Thus, these results show the potential for underwater laser imaging to be used for detecting garbage in water bodies such as oceans. In future work, we plan to work more on advanced deep learning-based image enhancement and object classification algorithms as well as design a prototype underwater ROV for finding and cleaning up ocean garbage.

## MATERIALS AND METHODS

All the experiments were conducted in a lab at the University of Alabama. Appropriate eye safety precautions were utilized to prevent any harm to human health. The test set-up consists of a 1.2 m x 0.3 m glass aquarium mounted on a table. In this way, imaging up to a depth of 1.2 m can be tested. A green laser with a wavelength of 532 nm was utilized with a beam expander to illuminate an object through the side of the water tank **(Figure 7)**. A filter was placed in front of the camera to only allow the frequency of the green laser to be detected by a camera. Although high-quality cameras are available for use as a detector, in this work, a personal cell phone was utilized as a cost-effective solution. To be able to capture as much of the object as possible, it was very important for the camera to be flush against the optical filter. Tinkercad was used to design and print a holder for the cell phone that could be inserted into an optical base upon which a cylindrical holder was screwed. The cell phone was then remotely controlled from a computer to enable visualization and acquisition of the laser image of objects.

In natural bodies of water, the water is oftentimes not clear but turbid due to the mixture of mud, sand, and biological materials in the water. In this work, the turbidity of the water in the tank was adjusted by mixing in calcium bentonite, a white powdery substance. We added 2 Tbsp of calcium bentonite into the water tank to get a concentration of approximately 0.23 g/L. A homogeneous distribution was ensured by using an aquarium pump in the tank to circulate the water.

The turbidity level in the water tank was measured by constructing a turbidity sensor utilizing a DfRobot turbidity sensor, Arduino Nano, 16x2 12C LCD display, breadboard, wires, solder, and soldering iron **(Figure 8)**. The turbidity sensor was wired to the Arduino Nano, using solder to form connections at places for which there was no connector. We modified code for operating the sensor posted at *how2electronics.com* to enable proper thresholding and calibration for different liquids. We found that with the original version of the code, the turbidity readings did not change for different liquids (e.g., water versus black tea). This was because a hard limit of 2.5 V had been utilized, which resulted in the constant saturation of values. With our modified code, the sensor values changed according to the transparency and turbidity of the liquid **(Figure 8)**. The sensor was calibrated so that tap water showed a reading of 0 Nephelometric Turbidity Units (NTU).

Experiments were conducted by imaging daily objects that might one day end up as ocean trash. A metal chain, almond milk bottle, small plastic shoes, a plastic beverage bottle,

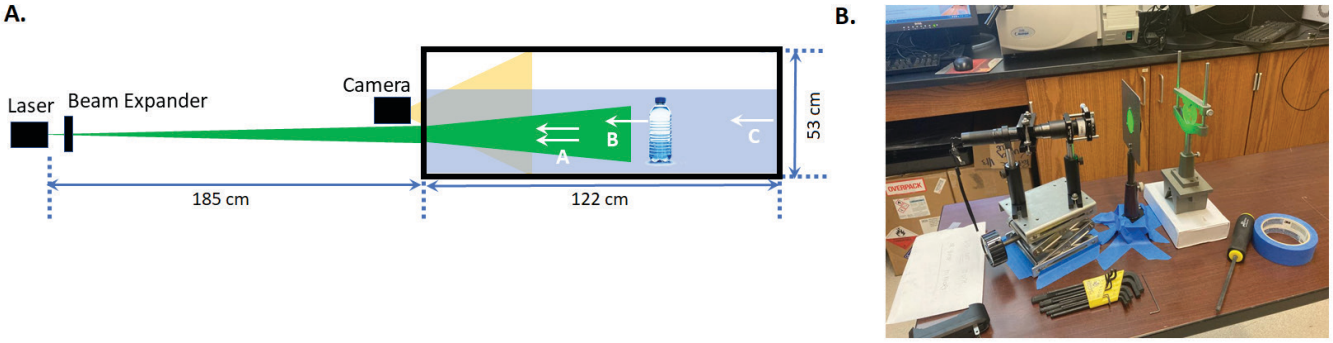


**Figure 7: Schematic of water tank test set up for underwater imaging experiments and laser with beam expander. A)** Objects placed in the water tank are illuminated by a laser whose beam is dispersed in the water before a camera captures the backscattered light from the object. **B)** Beam expanders are used to widen the laser beam so that the entire object is illuminated.

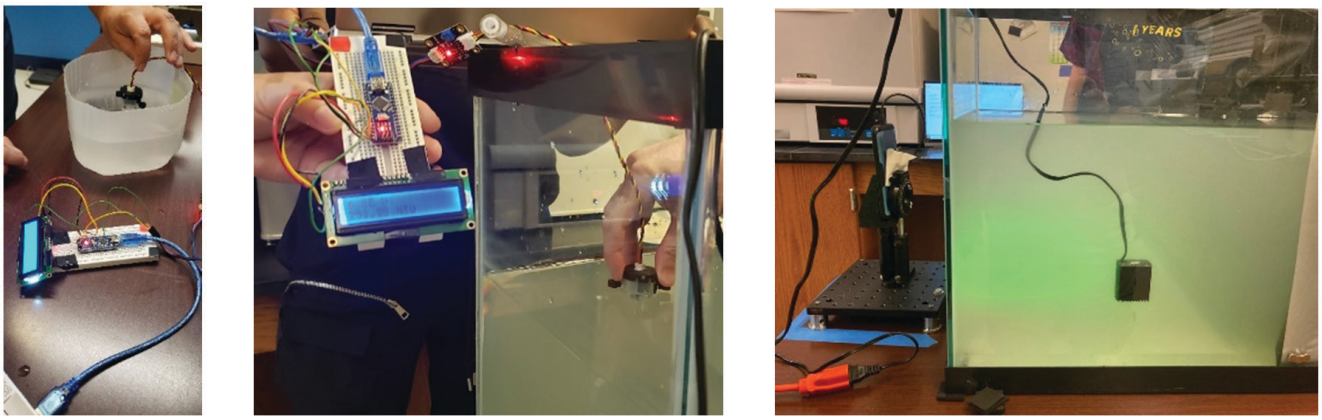


**Figure 8: Impact of turbidity on laser beam. A)** Measurement of turbidity of clear water (NTU=72) which establishes the baseline NTU value of our sensor. B) Measurement of turbidity of cloudy water (NTU=251) showing the result of adding calcium bentonite to water. C) Turbid water illuminated by laser. When turbidity is high, the particulates in the water cause great dispersion of the laser beam reducing the depth that it can penetrate.

an egg carton, and shoelaces were utilized. These objects were selected because of their variety in shapes, material, texture, color, shape, and inclusion of text (in the case of the bottles and carton). The richness of features would enable a better qualitative and quantitative evaluation of laser imaging efficacy. Four different experiments were conducted: 1) laser set to linear polarization, clear water in tank; 2) laser set to circular polarization, clear water in tank; 3) laser set to linear polarization, turbid water in tank; and 4) laser set to circular polarization, turbid water in tank.

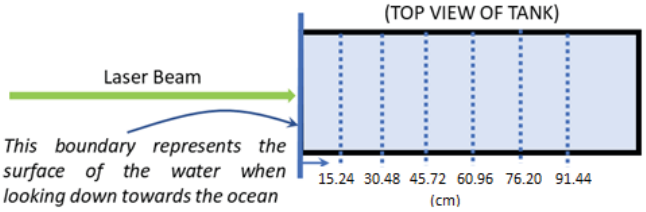


**Figure 9: Depth adjustment by placing objects at different distances from side of the tank.** Objects are placed at different distances from the glass wall of the tank to test the effect of depth on image resolution.

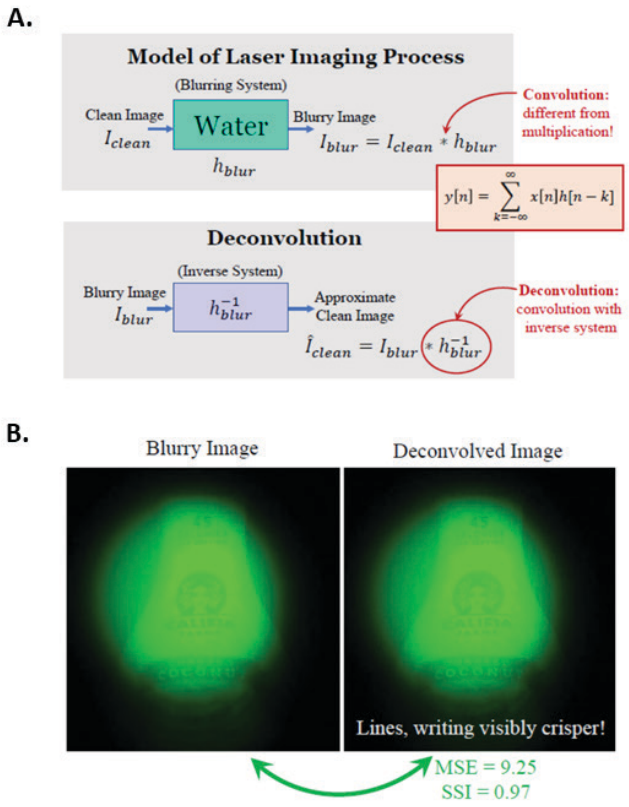


**Figure 10: Blind deconvolution impact on image clarity. A)** Concept of blind deconvolution for the removal of the effect of the water column. The block diagram shows the mathematical calculation done to invert the model of the water. **B)** Comparison of laser images before and after blind deconvolution. This example shows that blind deconvolution results in clearer images than other image processing techniques evaluated.

Additionally, during each experiment, the position of the object was moved towards the side of the tank most distant from the laser in 15.24 cm intervals. Moving the objects laterally within the tank at a position of 15.24 cm, 30.48 cm, 45.72 cm, 60.96 cm, 76.2 cm, and 91.44 cm from the near side of the tank effectively emulates water depths of those distances **(Figure 9)**.

We quantified the impact of depth and polarization on the quality of the laser images acquired, which were then evaluated using MSE and SSI image quality metrics. Each object, $I_0$, was defined as the image taken at 15.24 cm and $I_x$ as the images taken at 30.48, 45.72, 60.96, 76.2, or 91.44 cm depths. The MSE and SSI are then computed and plotted as a function of $\Delta$d, the difference in depth for both linear and circular polarizations. The trend over depth is compared to evaluate which is more effective. We also compared MSE and SSI values to evaluate deblurring algorithms: 1) Guided filtering, a noise reduction technique that preserves the edge details of the image by using the content in a second, guidance image to influence the filtering; 2) Dehazing, an approach originally designed for removing the effect of atmospheric haze, based on approximating the dark channel prior method using the local patches in a haze-free outdoor image that have very low intensity values in at least one-color channel; 3) Blind deconvolution, a method that models the blurry image as the convolution of a clear image with a model of the cause of the blurriness – in our case, the backscatter from the water. Convolution is the process for computing the output of a linear, time-invariant system given an input x[n] and an impulse response function h[n] that models the corrupting system **(Figure 10)** (38). If the water column is modeled as a blurring system with impulse response $h_{blur}$, then the blurry image is computed as $I_{blur}=I_{clean}*h_{blur}$, where * is the convolution operator. The effect of the water column can be removed if we know the inverse system $h_{blur}^{-1}$. Blind deconvolution refers to the case when the inverse is unknown (39). We assumed a generic Gaussian function to model the blurring system and manually adjusted the width of the function according to what visually gave the clearest looking image.

**Received:** June 6, 2022
**Accepted:** May 30, 2023
**Published:** July 7, 2023

## REFERENCES

1. "Marine & Ocean Pollution: Statistics & Facts 2020–2021." *Condorferries.co.uk,* 2022, www.condorferries.co.uk/marine-ocean-pollution-statistics-facts. Accessed 8 Dec 2022.
2. Pabortsava, Katsiaryna and Richard S. Lampitt. "High concentrations of plastic hidden beneath the surface of the Atlantic Ocean." *Nature Communications,* vol. 11, 2020. doi:10.1038/s41467-020-17932-9
3. "Ocean Pollution: 11 Facts You Need to Know." *Conservation International,* www.conservation.org/stories/ocean-pollution-11-facts-you-need-to-know. Accessed 15 Apr 2023.
4. "The Problem of Plastic Pollution: 100 Million Animals Killed Each Year," *Planet Love Life,* www.planetlovelife.com. Accessed 15 Apr 2023.
5. Zhang, Kai, *et. al,* "Understanding plastic degradation and microplastic formation in the environment: A review,"

*Environmental Pollution,* vol. 274, no. 116554, 2021. doi:10.1016/j.envpol.2021.116554
6. Wang, Yi, *et. al,* "Biodegradable microplastics: A review on the interaction with pollutants and influence to organisms," *Bull Environ. Contam. Toxicol.,* vol. 108, no. 6, 2022, pp. 1006-1012. doi:10.1007/s00128-022-03486-7
7. O'Neill, Claire, "How soda caps are killing birds," *The Picture Show: Photo Stories from NPR,* November 1, 2011.
8. Andrews, Gianna, "Plastics in the Ocean Affecting Human Health," serc.carleton.edu/NAGTWorkshops/health/case_studies/plastics.html. Accessed 15 Apr 2023.
9. Thielemann, Jens, *et. al,* "Developing and underwater 3D camera with range-gated imaging," *Mathworks Technical Articles and Newsletters,* 2019.
10. Hou, Weilin, "Active underwater imaging." *Ocean Sensing and Monitoring: Optics and Other Methods,* SPIE, 2013.
11. Han, Jing, *et. al,* "Simulated research on passive sonar range using different hydrographic conditions," *MATEC Web of Conferences,* vol. 35, no. 04003, 2015. doi:10.1051/matecconf/20153504003
12. Cho, Hyeonwoo, *et. al,* "Robust Sonar-Based Underwater Object Recognition Against Angle-of-View Variation," *IEEE Sensors Journal,* vol. 16, no. 4, pp. 1013-1025, Feb.15, 2016. doi:10.1109/JSEN.2015.2496945
13. Potenza, Alessandra, "Navy sonar that harms whales and dolphins was improperly approved, US court finds," *The Verge,* July 18, 2016.
14. EarthTalk, "Does military sonar kill marine wildlife? The frequency used in military testing could be harmful to some animals," *Scientific American,* June 10, 2009.
15. Parsons, E.C.M, "Impacts of navy sonar on whales and dolphins: Now beyond a smoking gun?" *Frontiers in Marine Science,* September 13, 2017.
16. Derbyshire, David, "Sonar soundwaves' drive terrified whales to their death onshore," *The Daily Mail,* March 15, 2011.
17. Dalgleish, Fraser, *et. al,* "Undersea LiDAR imager for unobtrusive and eye safe marine wildlife detection and classification," *OCEANS-Europe Conference,* 2017.
18. Filisetti, Andrew, *et. al,* "Developments and applications of underwater LIDAR systems in support of marine science," *OCEANS 2018 MTS/IEEE Charleston,* 2018. doi:10.1109/OCEANS.2018.8604547.
19. Scholz, Thomas, "Laser based underwater communication experiments in the Baltic Sea," *Fourth Underwater Communications and Networking Conference (UComms),* 2018.
20. Sen, Daqi, *et. al,* "Disruptive Technology of Building internet of Underwater Thigs: Laser-based underwater Solid-State Lighting," *5th IEEE Electron Devices Technology & Manufacturing Conference (EDTM),* 2021. doi:10.1109/EDTM50988.2021.9420948.
21. Woodward, Bryan, *et. al.,* "Underwater speech communications with a modulated laser," *Appl. Phys.,* vol. B 91, pp. 189–194, 2008.
22. Barat, Ken. "Lasers under the Sea.", *Laser Safety in Specialized Applications,* edited by Ken Barat, AIP Publishing, Melville, New York, 2021: 12-1
23. Zorn, Heather, *et. al.* "Laser safety thresholds for cetaceans and pinnipeds." *Marine Mammal Science,* vol. 16, no. 1, 2000, pp. 186-200. doi:10.1111/j.1748-7692.2000.tb00912.x
24. McManamon, Paul, "LIDAR Range Equation." *LIDAR Technologies and Systems,* SPIE, 2019
25. Dubrovinskaya, Elizaveta, *et. al,* "Underwater LIDAR Signal Processing for Enhanced Detection and Localization of Marine Life," *OCEANS - MTS/IEEE Kobe Techno-Oceans (OTO),* 2018.
26. Risholm, Petter, *et. al,* "High-resolution structured light D sensor for autonomous underwater inspection," *OCEANS 2018 MTS/IEEE Charleston,* 2018, pp. 1-5.
27. Albiez, Jan, "Kraken Robotic's SeaVision," *NOAA Ocean Exploration Logs,* 2019 Technology Demonstration, July 30, 2019.
28. Yang, Shu-bin, "Underwater Laser Imaging Target Detection Technology," *First Int. Conf. on Intelligent Networks and Intelligent Systems,* Wuhan, China, 2008, pp. 437-440.
29. Shen, Ying, "Underwater Optical Imaging: Key Technologies and Applications Review," in *IEEE Access,* vol. 9, pp. 85500-85514, 2021.
30. Sahu, Geet, *et. al,* "Trends and Prospects of Techniques for Haze Removal From Degraded Images: A Survey," *IEEE Transactions on Emerging Topics in Computational Intelligence,* vol. 6, no. 4, Aug. 2022, pp. 762-782. doi:10.1109/TETCI.2022.3173443.
31. Kashani, Alireza. "A Review of LIDAR Radiometric Processing: From Ad Hoc Intensity Correction to Rigorous Radiometric Calibration." *Sensors,* vol. 15, no. 11, 2015, pp. 28099-28128. doi:10.3390/s151128099
32. "Image Quality Metrics," *Mathworks,* www.mathworks.com/help/images/image-quality-metrics.html. Accessed 15 Apr 2023.
33. Sara, Umme, *et al,* "Image Quality Assessment through FSIM, SSIM, MSE and PSNR—A Comparative Study." *J. Computer and Communications,* vol.7, no.6, March 2019, pp. 8-18. doi:10.4236/jcc.2019.73002
34. "Image Deblurring," *Mathworks,* www.mathworks.com/products/image.html#impre. Accessed 15 Apr. 2023.
35. He, Kaiming, *et. al,* "Guided Image Filtering." *IEEE Transactions on Pattern Analysis and Machine Intelligence,* vol. 35, no. 6, June 2013, pp. 1397-1409. doi:10.1109/TPAMI.2012.213
36. He, Kaiming, *et. al,* "Single image haze removal using dark channel prior," *IEEE Conf. on Computer Vision and Pattern Recognition,* 2009, pp. 1956-1963.
37. Verman, Gunjan, *et. al,* "Systematic review and analysis on underwater image enhancement methods, datasets, and evaluation metrics," *Journal of Electronic Imaging,* vol. 31, no. 6, November 8, 2022. doi:10.1117/1.JEI.31.6.060901
38. A.V. Oppenheim, A.S. Willsky, S. Nawab, "Signals and Systems," Pearson, 1996.
39. "Blind Deconvolution," *Mathworks,* www.mathworks.com/help/images/ref/deconvblind.html. Accessed 15 Apr 2023.